CORROSION SCIENCE AND TECHNOLOGY, Vol.6, No.3(2007), pp.103~111

Consideration of Methods Evaluating the Growing Process of Stress Corrosion Cracking of the Sensitized 18-8 Austenitic Stainless Steel in High Temperature Water Based on Electric Circuit Theory: The Effects of Stress Factors

Yasoji Tsukaue

1-28-26-204 Higashi-terao, Tsurumi-ku, Yokohama-shi, Kanagawa-ken, 230-0077 Japan

The effect of stress factors on the growing process of stress corrosion cracking (SCC) of the sensitized 18-8 stainless steel in high temperature water was investigated using equations of crack growth rate derived from applying electric circuits to SCC corrosion paths. Three kinds of cross sections have to be considered when electric circuit is constructed using total current. The first is ion flow passage area, S_{sol}, of solution in crack, the second is total dissolving surface area, S_{dis}, of metal on electrode of crack tip and the third is dissolving cross section, S_{met}, of metal on grain boundary or in base metal or in welding metal. Stress may affect each area. S_{sol} may depend on applied stress, σ_∞, related with crack depth. S_{dis} is expressed using a factor of ε(K) and may depend on stress intensity factor, K only. SCC crack growth rate is ordinarily estimated using a variable of K only as stress factor. However it may be expected that SCC crack growth rate depends on both applied stress σ_∞ and K or both crack depth and K from this consideration.ε(K) is expressed as $\varepsilon(K)= h_2 \cdot K^2 + h_3 \cdot K^3$ when h_2 and h_3 are coefficients. Also, relationships between SCC crack growth rate, da/dt and K were simulated and compared with the literature data of JBWR-VIP-04, NRC NUREG-0313 Rev.2 and SKIFS Draft. It was pointed out in CT test that the difference of distance between a point of application of force and the end of starter notch (starting point of fatigue crack) may be important to estimate SCC crack growth rate. An anode dissolution current density was quantitatively evaluated using a derived equation.

Keywords *: electric circuit, stress corrosion cracking, sensitized 18-8 austenitic stainless steel, high temperature water, growing process*

1. Introduction

Author has been quantitatively considered the methods of evaluating the growth process of stress corrosion cracking (SCC) of the sensitized 18-8 austenitic stainless steel in high temperature water applying an electric circuit theory to the multiple corrosion paths of a crack.[1),2)] To apply an electric circuit theory to SCC growth process has such several advantages that the calculated anode circuit current shows directly the crack growth rate of SCC and many information such as metallic and fracture-mechanical parameters at crack tip, electrochemical parameters on anode and cathodes in crack inside and outside and hydrolysis reaction parameters in crack solution as three elements of material, stress and environment of SCC can be introduced in the circuit current equation. On the other hand, many researchers have measured the crack growth rate of 18-8 stainless steel in high temperature water using several testing methods and estimated it using stress intensity factor, K up to now.[3)] However the measured data base for sensitized Type 304 stainless steel in BWR environment extends to about 6 order ranges of 10^{-12} to 10^{-6} m/s to the same K value.[3)] In this paper, the relationship between crack growth rate and three kinds of the flowing areas affecting circuit current or current resistance are considered from the standpoint of stress factors, and effects of crack depth, l_{sol}, applied stress,σ_∞ and K on crack growth rate of the sensitized 18-8 austenitic stainless steel in high temperature water are quantitatively estimated using the equations derived by electric circuit theory.

† Corresponding author: y.tsukaue@r2.dion.ne.jp

2. Mathematical model

2.1 Conditions of crack model

Fig. 1 shows a model of SCC crack geometry and flows of electrons and various ions in the neighborhood of the

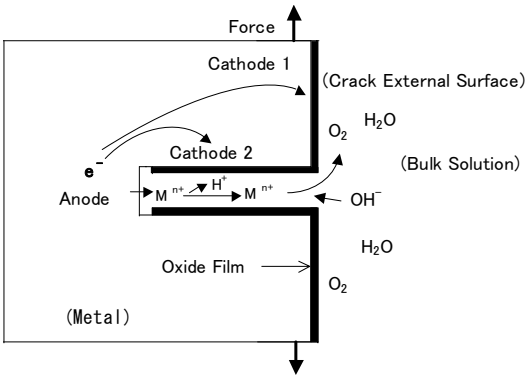

Fig. 1. SCC crack geometry and flows of electrons and various ions in the neigh-borhood of the crack as corrosion paths

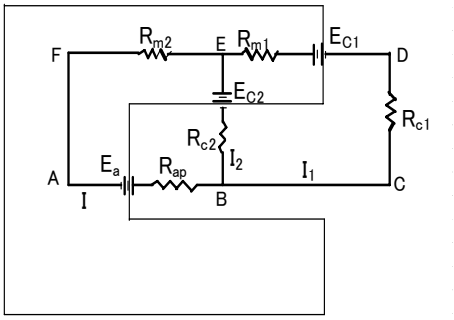

Fig. 2. Electric circuits constituted of circuit 1 and circuit 2 simulated the flow of electron and various ions shown in Fig. 1

crack. In this paper, it is assumed that only the crack tip is bare and the other surfaces are covered by oxide film as shown in Fig.1 and the metal compositions of the sensitized 18-8 austenitic stainless steel dissolved into crack solution at crack tip is the same as that of the sensitized matrix at crack tip. Cr^{3+} ions only is considered regarding hydrolysis reaction in crack solution because the equilibrium constant is remarkably larger than those of other metallic ions.[2] It is also assumed that H^+ ions produced near the crack tip are reduced at the central zone of sidewalls in crack. Fig. 2 shows an electric circuit network with two electric circuits corresponding to two corrosion paths as shown in Fig.1. In Fig. 2 circuit 1 is a closed circuit of A-B-C-D-E-F-A and the anode is on crack tip and the cathode is on crack entrance surface (cathode 1). On the other hand circuit 2 is a closed circuit of A-B-E-F-A and the anode is on crack tip and the cathode is on crack sidewall surface (cathode 2). It is assumed that Kirchhoff's laws can be applied to these electric circuits.

2.2 Equations of crack growth rate

Total circuit current, I which flows through the surface of crack tip can be mathematically derived from circuit equations produced according to Fig. 2 and crack growth rate, da/dt can be expressed as follows.[1),2)]

$$\frac{da}{dt}=\frac{M}{n\times F\times S\times \rho}\times I=\frac{M}{n\times F\times S\times \rho}\times\left(f\times C_{M^{n+}}+g_2\times C_{H^+}\right) \quad (1)$$

where C_{Mn+} and C_{H+} are total metallic ion concentration and hydrogen ion concentration in crack solution respectively. parameters of f and g_2 can be expressed using dissolution parameter, $\varepsilon(K)$, as follows.

$$f=\frac{a_0}{1+\dfrac{a_1}{\varepsilon(K)}} \quad \text{and} \quad g_2=\frac{b_0}{1+\dfrac{b_1}{\varepsilon(K)}} \quad (2)$$

When da/dt is calculated using Eqs. 1 and 2, three areas of S_{sol}, S_{dis} and S_{met} as shown in Fig. 3 must be determined. S_{sol} is ion flow passage area of solution in crack, S_{dis} is total dissolving surface area of metal on electrode of crack tip and S_{met} is dissolving cross section of metal on grain boundary or in base metal or in welding metal. Eq. 1 can be expressed as follows using S_{sol}, S_{dis} and S_{met}.

$$\frac{da}{dt}=\frac{M}{n\times F\times \rho\times S_{met}}\times\frac{S_{sol}}{l_{sol}}\left[\frac{a_0^{'}}{1+\dfrac{a_1}{S_{dis}/S_{a0}}}\times C_{M^{n+}}+\frac{b_0^{'}}{1+\dfrac{b_1}{S_{dis}/S_{a0}}}\times C_{H^+}\right] \quad (3)$$

where l_{sol} is a distance of crack tip to crack entrance between which ions move in crack solution and corresponds to crack depth. If width of crack tip depends on crack tip opening displacement (CTOD) of δ, S_{met} or S_{sol} can be expressed by next equation under plane strain condition when B_{CT} is crack length.[4)]

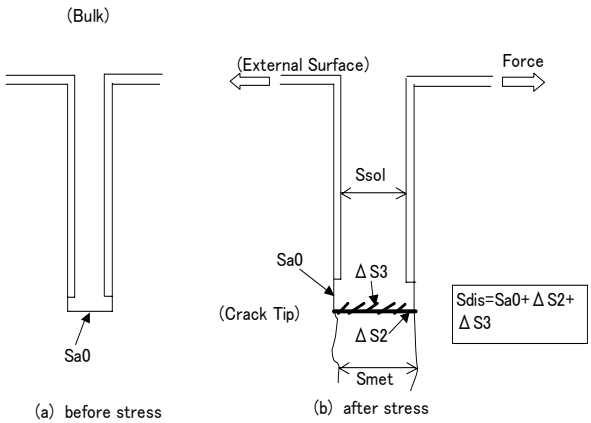

Fig. 3. A modeling of SCC crack tip before stress and after stress as to various area.

$$S_{met} \text{ or } S_{sol} = B_{CT} \times K^2 / 2\sigma_y E \quad (4)$$

Also dissolution parameter, ε(K) is shown as follows using the area of S_{dis} when ΔS is defined as dissolution area increased by stress at the surface of crack tip.

$$\varepsilon(K) = S_{dis} / S_{a0} = 1 + \Delta S / S_{a0} \quad (5)$$

In Fig. 3, ΔS_2 is two-dimensional area formed by action of stress and depends on CTOD. On the other hand, ΔS_3 is three-dimensional area formed on ΔS_2 by strain. Dissolution area increment, ΔS which is formed on crack tip by action of stress is expressed as a sum of ΔS_2 and ΔS_3. Therefore total dissolution area, S_{dis} is expressed by next equation.

$$S_{dis} = S_{a0} + \Delta S_2 + \Delta S_3 \quad (6)$$

In this paper, it is assumed that S_{a0} after stress as shown in Fig. 3 is formed by plastic deformation of the sensitized matrix and mother metal of sidewalls near crack tip are not corroded during crack propagation. Similarly, K dependence of ε(K) can be derived as follows.[5),6)]

$$\varepsilon(K_I) = 1 + \frac{B_{CT}}{2S_{a0}\sigma_y E} \times K^2 + \frac{B_{CT} B_X \sqrt{\overline{\varepsilon_C}}}{2 i_0 S_{a0} \sigma_y^2 E} \times K^3 \quad (7)$$

where i_0 is current density on crack tip in unstressed condition and both B_X and $\overline{\varepsilon_C}$ are constant related to strain. In what follows, the value of crack length of $B_{CT} = 0.1$ cm is used to estimate crack growth rate and so on.

2.3 Hydrogen ion concentration(C_{H+}) in crack

Hydrogen ion concentration, C_{H+} in crack described in Eq. 1 can be obtained using parameter, P_C defined by the following equation.[2)]

$$P_C = f - \delta_{Cr} \times K_{Cr} \times g_2 \quad (8)$$

where δ_{Cr} shows the ratio of amount of Cr to total metal amount at crack tip and K_{Cr} is an equilibrium constant in hydrolysis reaction of Cr^{3+} ions. In Eq. 8, in case of $P_C>0$, it can be understood from Eq. 2 that H^+ ion concentration, C_{H+} may increase regardless of presence or absence of stress or K. Also, in case of $P_C<0$, C_{H+} may decrease with time regardless of presence or absence of stress or K.

On the other hand, in case of $P_C = 0$, a constant pH can be determined as function of ε(K) depending on stress or K and it can be expected that this process of $P_C = 0$ corresponds to SCC growing process. Fig. 4 shows a diagram which shows a relationship between decreasing process of pH in crack and parameters of a_0 and $\delta_{Cr} \times K_{Cr} \times g_2$. In Fig. 4, it may be expected that the pH in crack decreases from neutral zone of ① to acid zone of ⑤ along pH axis with time. The regions of pattern I and III correspond to the conditions of $P_C>0$ and $P_C>0$ respectively. The region of pattern II corresponds to SCC growing process. The pH in crack may decrease up to a position of ③ in an unstressed condition when time has passed enough. Moreover, the pH can decrease from ③ to ④ if stress acts. The pH between ③ to ④ can be obtained by solving mathematically $P_C = 0$ in Eq. 8. Therefore, it may be expected that SCC crack growth rate, da/dt has a minimum value at a position of ③ and has a maximum value at a position of ④.

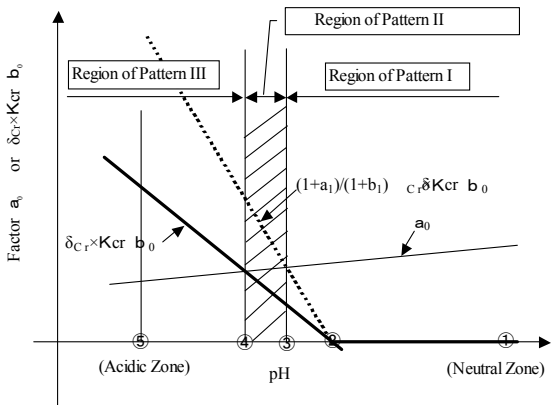

Fig. 4. A diagram which shows a relation between decreasing process of ph in crack and parameters of a_0 and $\delta_{Cr} \times K_{Cr} \times g_2$.

A condition of $0<b_1<a_1<1$ regarding parameters of a_1 and b_1 shown in Eq. 2 is necessary to be able to solve the equation of $P_C = 0$. If $a_1 = 1$ and $b_1 = 0$ are assumed, pH in SCC crack of the sensitized 18-8 stainless steel in 288 ℃ high temperature water can be derived as a function of ε(K) and δ_{Cr} as follows.

$$pH = \frac{(-6.30 + 97.7 \times \delta_{Cr})\,\varepsilon(K) + 97.7 \times \delta_{Cr}}{(0.47 + 12.5 \times \delta_{Cr})\,\varepsilon(K) + 12.5 \times \delta_{Cr}} \quad (9)$$

Hydrogen ion concentration, C_{H+} can be calculated from a relation of $C_{H+} = 10^{-pH}$ when C_{H+} is small and activity coefficient is nearly equal to 1.

3. Results and discussion

3.1 A Relationship between pH in crack and K

Fig. 5 shows a K dependence of pH in crack calculated using Eqs. 7 and 8 regarding SCC growing process of

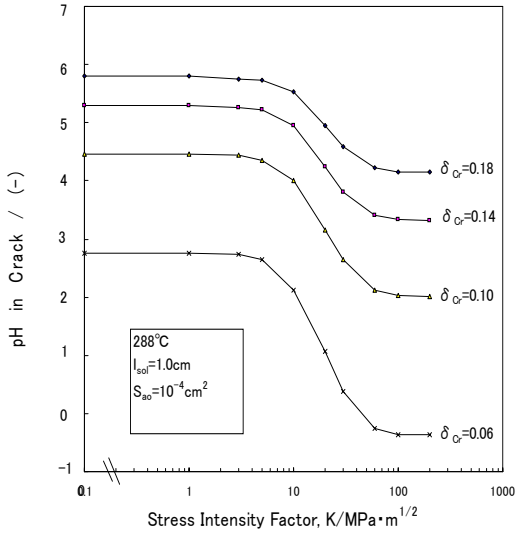

Fig. 5. K dependence of pH in crack calculated using Eqs. 7 and 8 in 288℃ high temperature water.

the sensitized 18-8 stainless steel in high temperature water under the conditions of $l_{sol} = 1.0$ cm and $S_{a0} = 10^{-4}$ cm^2. The pH in crack becomes lower as the degree of sensitization becomes greater, namely δ_{Cr} becomes smaller. Also the pH in crack is nearly constant to K of 0 to 5 MPa · m$^{1/2}$ and becomes rapidly lower near K of 10 MPa · m$^{1/2}$ and saturates over K of 60 MPa · m$^{1/2}$. It may be expected that this tendency of K dependence of pH causes similar effects to K dependence of SCC crack growth rate. In Fig. 5, the fluctuation range of pH in crack regarding δ_{Cr} of 0.18, 0.14, 0.10 and 0.06 is about 2, 2.5 and 3 respectively. It has a tendency to increase as δ_{Cr} becomes smaller or degree of sensitization becomes greater. Since the fluctuation range of pH regarding δ_{Cr} of 0.18, 0.14 and 0.10 corresponds to C_{H+} change of about 100 times, 300 times and 1000 times respectively, it may be expected that the change of pH in crack affects remarkably SCC crack growth rate. The threshold value of pH at which oxide film exists stably on the sensitized 18-8 stainless steel in 288 ℃ high temperature water is about 2.0 over the potential of 0 V(SHE) and it may arise over 2.0 when the potential is below 0 V(SHE).[7] Therefore, it may be expected that the oxide film on 18-8 stainless steel with δ_{Cr} of 0.10 and 0.06 in 288 ℃ high temperature water becomes unstable or dissolved at K values of 100 MPa · m$^{1/2}$ and 10 MPa · m$^{1/2}$ respectively and the corrosion form changes from SCC to general corrosion or intergranular corrosion.

3.2 A relationship between da/dt and K

3.2.1 In case S_{met} is equal to S_{sol} :

(1) Effect of Cr conposition, (δ_{Cr})

In case S_{met} is equal to S_{sol}, SCC crack growth rate, da/dt can be obtained from Eq. 10 as follows.

$$\frac{da}{dt} = \frac{M}{n \times F \times \rho} \times \frac{1}{l_{sol}} \left[\frac{a_0'}{1 + \frac{a_1}{S_{dis}/S_{a0}}} \times C_{M^{n+}} + \frac{b_0'}{1 + \frac{b_1}{S_{dis}/S_{a0}}} \times C_{H^+} \right] \quad (10)$$

In this case, SCC crack growth rate, da/dt depends on stress intensity factor, K as stress factors through parameters of l_{sol} and S_{dis} as described in Eq. 10. The crack depth of l_{sol} is related to stress factor as configuration factor of K. In what follows, it is assumed that total metallic ion concentration in crack, C_{Mn+} is equal to 5 times that of hydrogen ions in crack in calculating the da/dt because it can be expected that all of the dissolved chrome atoms containing about 10% to 20% of the sensitized matrix metal change to hydrogen ions by reason of remarkably large equilibrium constant of over one in hydrolysis reaction of Cr^{3+} ions in 288 ℃ high temperature water.

Fig. 6 shows K dependence of da/dt regarding various δ_{Cr} under the conditions of $l_{sol} = 1.0$ cm and $S_{a0} = 10^{-4}$ cm^2 in 288 ℃ high temperature water containing 200 ppb O_2. In Fig. 6, the calculated da/dt vs. K curves regarding $\delta_{Cr} = 0.16$ and $\delta_{Cr} = 0.18$ is nearly equal to a guideline curve to low carbon stainless steel shown in the literature of JBWR-VIP-04.[8] Similarly, the calculated da/dt vs. K curve regarding $\delta_{Cr} = 0.14$ is nearly equal to a guideline curve to the sensitized SUS304 stainless steel shown in the same literature. Also, the guideline curves for estimation of SCC crack growth rate of the sensitized 18-8 stainless steel in the literatures of NRC NUREG-0313 Rev.2

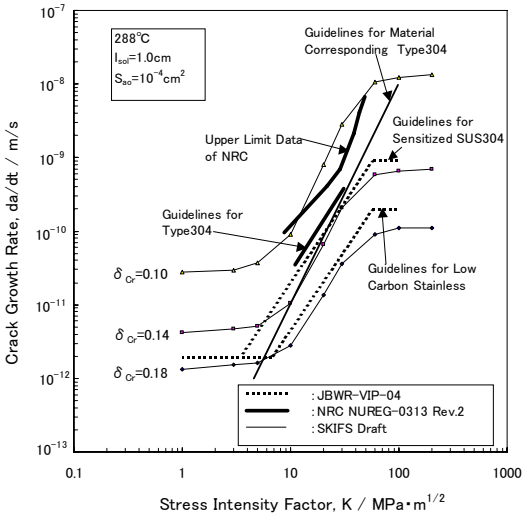

Fig. 6. Relationships of the calculated crack growth rate and K regarding various δ_{Cr} and the comparison with various guidelines

and SKIFS Draft are shown in Fig. 6.[9] Crack growth rate of step I of SCC propagation characteristics of the sensitized stainless steel depends on $K^{2.161}$ in NRC NUREG-0313 Rev.2 and depends on K^3 in SKIFS Draft. On the other hand, crack growth rate derived from electric circuit theory may depend on a sum of K^2 and K^3 as expected from Eq. 7. The calculated curve regarding $\delta_{Cr} = 0.10$ is remarkably larger than those of these guideline curves, but it is near the upper limit of da/dt vs. K data shown in NRC NUREG-0313 Rev.2. In previous section, it was discussed that the oxide film on metal in 288℃ high temperature water may be unstable in case pH in crack attains to about 2 at enough larger K value regarding$\delta_{Cr} = 0.10$. Namely it may be expected that the calculated da/dt vs. K curve regarding $\delta_{Cr} = 0.10$ and the upper limit data of NRC NUREG-0313 Rev.2 are located on the upper limit region of SCC growth process under the conditions. Also, it can be understood from Fig. 6 that the changes of da/dt regarding δ_{Cr} of 0.18, 0.14 and 0.10 are 90 times, 170 times and 500 times when K changes from 1 to 200 MPa · $m^{1/2}$. The calculated crack growth rate in Fig. 6 is nearly constant up to K of about 5 MPa · $m^{1/2}$ and tends to saturate over K of about 60 MPa · $m^{1/2}$. It may be expected that this saturation depends on δ_{Cr}, K_{Cr} and normal electrode potential at each anode and cathode from Eq. 9.

(2) Effects of SCC crack depth, l_{sol}

Fig. 7 shows K dependence of SCC crack growth rate, da/dt calculated using the Eq. 10 regarding a parameter of crack depth, l_{sol} under the conditions of $\delta_{Cr} = 0.18$ and $S_{a0} = 10^{-4}cm^2$ in 288 ℃ high temperature water containing 200 ppb O_2 · SCC crack growth rate decreases in inverse proportion to crack depth and the ratio of decrease in crack growth rate becomes smaller as crack depth increases as shown in Eq. 10. Crack growth rate increases 30 times when l_{sol} changes from 0.1 cm to 3.0 cm.

(3) Temporal change in crack depth

It is difficult to expect quantitatively a time dependence of SCC crack depth, l_{sol} since it can be considered that K remarkably changes with crack propagation in the region of small crack depth and it influences crack growth rate as understood in Eq. 10. However, in the growing stage with enough crack depth, l_{sol}, K is regarded as a constant to small changes of crack. In this case, as the variable of da/dt regarding time is l_{sol} only, Eq. 10 is expressed as follows when l_{sol} is replaced by $L_G+\Delta l_{sol}$ with large constant L_G.

$$\frac{d\Delta l_{sol}}{dt} = \frac{C_0(K)}{L_G + \Delta l_{sol}} \tag{11}$$

where $C_0(K)$ is a coefficient depending on K. The following equation is derived from Eq. 11.

$$\Delta l_{sol} = L_G\left(\sqrt{1+\frac{2C_0(K)\times t}{L_G^2}} - 1\right) \tag{12}$$

Eq. 12 shows that Δl_{sol} changes linearly to time when L_G is large and on the other hand it draws a parabolic curve when LG is small. Fig. 8 shows time dependence of Δl_{sol} regarding K under the conditions of $\delta_{Cr} = 0.18$ and $L_G = 1.0$ cm.

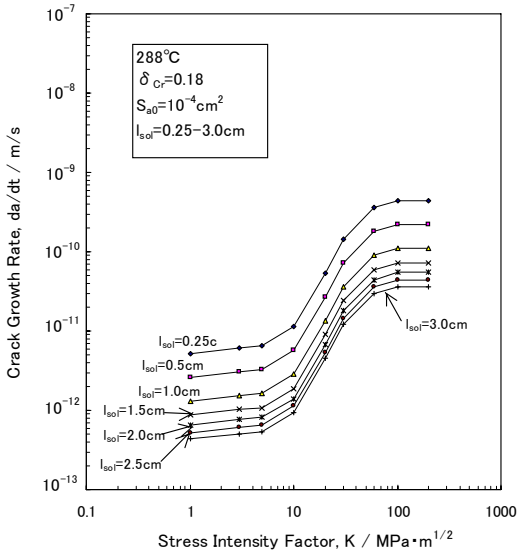

Fig. 7. K dependence of the calculated crack growth rate regarding various SCC crack depth, l_{sol}.

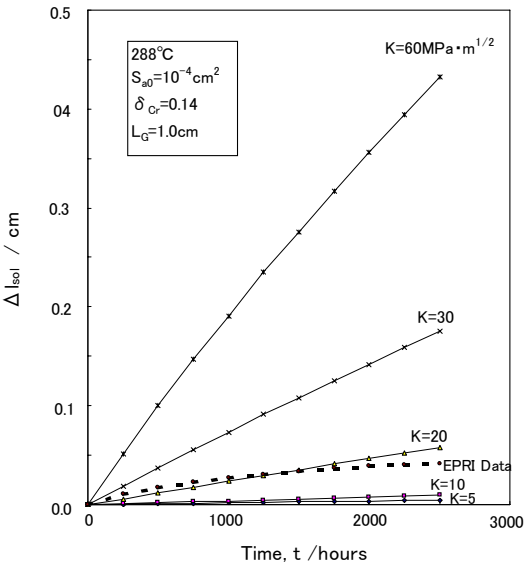

Fig. 8. Time dependence of Δl_{sol} regarding K under the conditions of δ_{Cr}=0.18 and L_G=1.0 cm

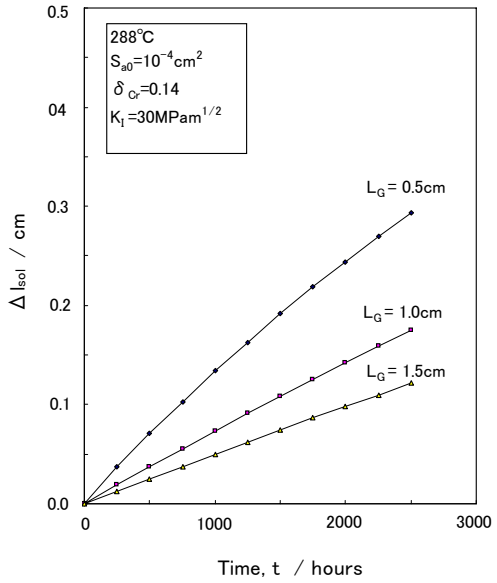

Fig. 9. Time dependence of Δlsol regarding L_G under the conditions of δ_{Cr}=0.14, $S_{a0}=10^{-4}$ cm^2 and K=30 MPa · $m^{1/2}$

The calculated results show nearly linear change and Δl_{sol} becomes large as K is large. The dashed line in Fig. 8 shows a literature data under BWR environment.[10] Also, Fig. 9 shows time dependence of Δl_{sol} regarding L_G under the conditions of $\delta_{Cr}=0.14$, $S_{a0}=10^{-4}cm^2$ and K = 30 MP a · $m^{1/2}$. The calculated Δl_{sol} changes linearly with time and the values of Δl_{sol} become larger as L_G is smaller and as a result, it can be understood that crack growth rate becomes larger. From the above consideration, it can be expected that in case a compact tension specimen (CT specimen) is used to a measurements of SCC crack growth rate, the difference of distance between a point of application of force and the end of starter notch (starting point of fatigue crack) may influence SCC crack growth rate. Suzuki et al. pointed out that SCC crack growth rate become faster when small specimen was used.[11]

3.2.2 In case of the fixed S_{met} :

Even if K changes or not, SCC crack growth rate of Eq. 1 may be expressed by the following equation using applied stress, σ_∞, yield stress, σ_y and Young's modulus, E in case dissolution area of metal matrix at crack tip, S_{met} is limited to a fixed extent perpendicular to the growing direction. In the case such as IGSCC of the sensitized 18-8 stainless steel, SCC propagation with the fixed S_{met} can be expected because the grain boundary region containing fewer chrome is corroded preferentially.

$$\frac{da}{dt}=\frac{M}{n\times F\times\rho\times S_{met}}\times\frac{B_{CT}\sigma_\infty^2}{2\sigma_y E}\times\left[\frac{a_0^{'}}{1+\frac{a_1}{S_{dis}/S_{a0}}}\times C_{M^{n+}}+\frac{b_0^{'}}{1+\frac{b_1}{S_{dis}/S_{a0}}}\times C_{H^+}\right] \quad (13)$$

Eq. 13 shows that SCC crack growth rate is proportional to the square power of applied stress, σ_∞ and is in inverse proportion to the product of yield stress, σ_y and Young's modulus, E. Fig. 10 shows the calculated results of applied stress dependence of da/dt regarding S_{met} of 1 μm and 10 μm according to Eq. 13 under the conditions of $\delta_{Cr}=0.18$, $S_{a0}=10^{-4}cm^2$ and $l_{sol}=1.0$ cm in 288 ℃ high temperature water. The values of applied stress, σ_∞ of $0.67\sigma_y$, $1.0\sigma_y$ and $1.5\sigma_y$ were considered in calculating da/dt. The values of da/dt regarding $S_{met}=1$ μm are larger than those regarding $S_{met}=1$ μm from Fig. 10. The da/dt increases as applied stress increases. Also, Fig. 11 shows the calculated results of da/dt vs. K as to $\delta_{Cr}=0.14$. It may be predicted that da/dt fluctuates about 100 times to K between 1 to

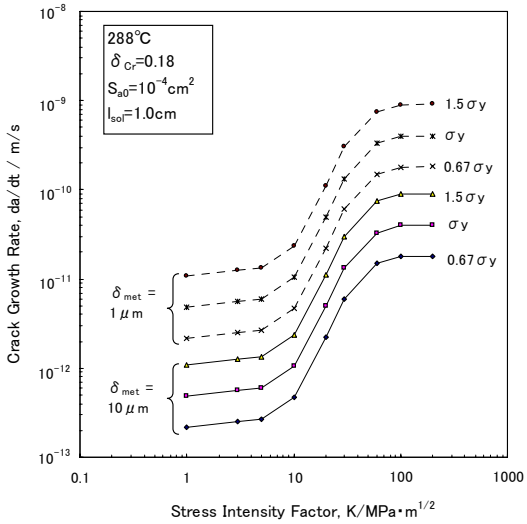

Fig. 10. The calculated results of K dependence of SCC crack growth rate regarding δ_{Cr}=0.18 in case of the fixed S_{met}.

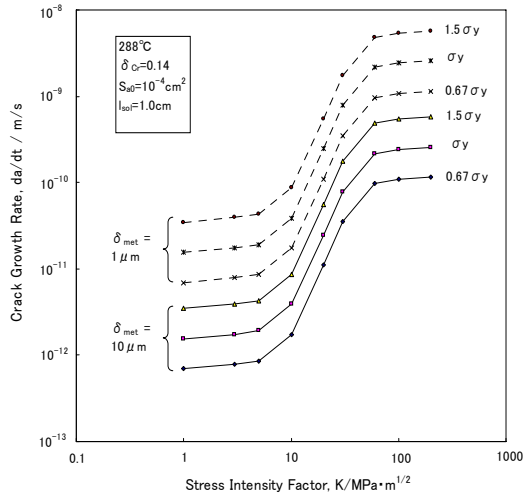

Fig. 11. The calculated results of K dependence of SCC crack growth rate regarding δ_{Cr}=0.14 in case of the fixed S_{met}.

200 MPa · $m^{1/2}$ regarding advance of sensitization and increase in applied stress under the condition of the fixed S_{met} as shown in Figs. 10 and 11.

3.2.3 Effects of S_{dis}

(1) K dependence of ΔS_2 and ΔS_3

The total dissolution area, S_{dis} at crack tip is expressed a sum of S_{a0} which does not depend on stress, ΔS_2 of 2-dimensional area which depends on K^2 and ΔS_3 of 3-dimensional area which depends on K^3 as described in section 2.2. Fig. 12 shows the calculated results of K dependence of ΔS_2 and ΔS_3 at crack tip of the sensitized 18-8 stainless steel in 288 ℃ high temperature water. It can be understood that the value of ΔS_2 is larger than that of ΔS_3 when K is less than about 15 MPa · $m^{1/2}$ and on the other hand, the value of ΔS_3 is larger than that of ΔS_2 when K is more than 15 MPa · $m^{1/2}$. The levels of initial area, S_{a0} of 10^{-5} cm^2, $10^{-4}cm^2$ and $10^{-3}cm^2$ were shown in Fig. 12.

In the previous sections, the calculation of da/dt was mainly performed regarding $S_{a0} = 10^{-4}cm^2$. In this case, it can be understood that dissolution surface area which depends on stress becomes larger than that which does not depend on stress when K is more than about 20 MPa · $m^{1/2}$.

(2) Effects of initial dissolution surface, S_{a0} on a relation of da/dt vs. K

The side walls near the crack tip may be almost bear and a value of parameter, S_{a0} may be not zero since it can be predicted that a solution near the crack tip is concentrated by the dissolved metal ions or hydrogen ions produced from hydrolysis reaction due to metallic ions and so on and dissolved oxygen is hardly contained in it.

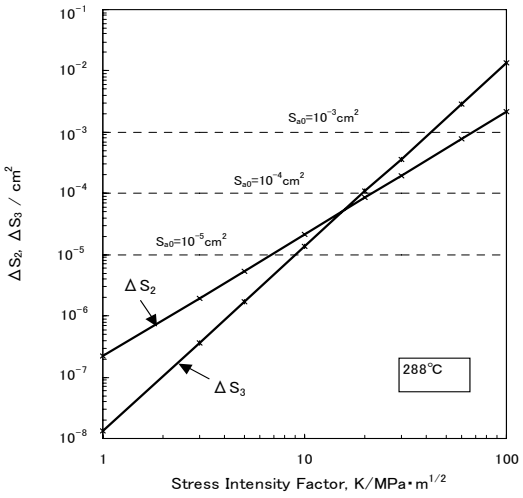

Fig. 12. The calculated results of K dependence of ΔS_2 and ΔS_3 in 288 ℃ high temperature water

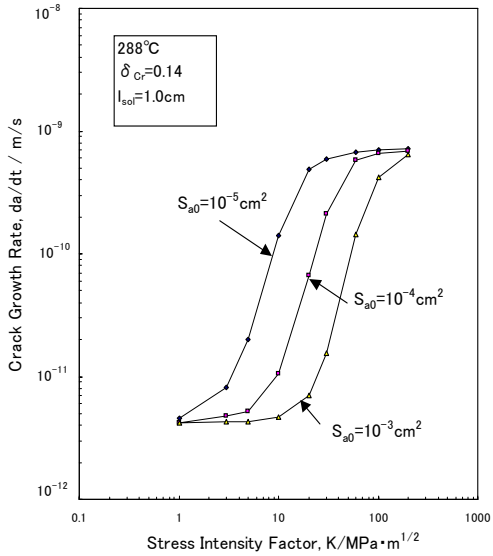

Fig. 13. Effects of S_{a0} on a relationship of da/dt vs. K under the condition of δ_{Cr}=0.14.

Fig. 13 shows effects of S_{a0} on a relationship of da/dt vs. K under the condition of $\delta_{Cr} = 0.14$. From Fig. 13, it can be understood that the values of lower limits or upper limits of da/dt are not affected even if da/dt increases with decrease in S_{a0}. It is not now clear experimentally what depends on S_{a0} regarding environmental factors. However, it may be expected that the dissolved oxygen concentration influences S_{a0} as it affects stability of oxide film. It is confirmed experimentally that crack growth rate of the sensitized 18-8 stainless steel increases with increase in dissolved oxygen concentration in high temperature water.[12] If the value of S_{a0} becomes small with dissolved oxygen concentration, it may be possible to explain the above experimental results using Eq. 3 as considered in Fig. 13.

(3) Effects of cold work on a relation of da/dt vs. K

It was reported that SCC crack growth rate showed a tendency of increase at the same K value under BWR Environment when low carbon stainless steel was cold worked.[13] When stainless steel was cold worked as pretreatment, an increase of yield stress and dislocation density is mainly expected to be arise from work hardening.

The increase in yield stress and dislocation density can influence the dissolution parameter, ε(K) according to Eq. 7. Namely, increase in yield stress may decrease da/dt and on the other hand increase in dislocation density may increase da/dt. The increase in dislocation density may increases surface defects and sites for dissolution[14] and as a results it influences a factor, Bx in Eq. 7 and da/dt may increase. N.Otani pointed out that in many metal dislocation density formed by cold work of 10% attains to

10^2 to 10^3 times that of annealed metal.[14] On the other hand, S. Suzuki et al. also reported that yield stress of 18-8 stainless steel in 288 ℃ high temperature water increases about 3 times.[11] Accordingly, it can be expected that a factor of Bx/σ_y^2 in Eq. 7 increases about 10 times compared from annealed metal. It may be expected that da/dt of 18-8 stainless steel increases on account of cold work as well as an increase in a coefficient of K in Eq. 10 raises a curve of da/dt vs. K from a curve as to $S_{a0} = 10^{-4}$ to a curve as to $S_{a0} = 10^{-5}$.

3.3 A relationship between dissolution current density, ia and K

Total current, I which dissolves from the surface area, S_{dis} at SCC crack tip of the sensitized 18-8 stainless steel in 288 ℃ high temperature water can be quantitatively expressed by the following equation.

$$I = \frac{S_{sol}}{l_{sol}}\left[\frac{a_0'}{1+\frac{a_1}{S_{dis}/S_{a0}}}\times C_{M^{n+}} + \frac{b_0'}{1+\frac{b_1}{S_{dis}/S_{a0}}}\times C_{H^+}\right] \quad (13)$$

Fig. 14 shows a K dependence of anode dissolution current density, i_a obtained by dividing the total current, I by initial surface, $S_{a0}(10^{-4}cm^2)$ at crack tip regarding δ_{Cr} of 0.18, 0.14 and 0.10 in 288 ℃ high temperature water. In Fig. 14, i_a becomes large as δ_{Cr} becomes small. On the other hand, i_a changes from the level of 10^{-8} to 10^{-7} A/cm^2 near exchange current density to the high level of 10^{-2} to 1 A/cm^2 at K value of 100 MPa · m$^{1/2}$. Hoar et al. considered that a remarkable decrease of activation polarization caused by action of stress from anode polarization measurements in boiling 42% $MgCl_2$ solution may arise from increase about 10^5 times in exchange current density.[15] Also, Hoar considered that a remarkable high anode current density of about 0.4 to 2.0 A/cm^2 occurs at SCC crack tip of austenitic stainless steel.[16] The calculated results of anode dissolution current density, i_a according to Eq. 13 at high K value is near to the above considered result by Hoar. On the other hand, peak current density is predicted to be about 10^{-4} to 10^{-3}A/cm^2 from measurements of anode polarization curves regarding 18-8 stainless steel in high temperature water near 288 ℃.[17),18] Therefore, the high current density shown in Fig. 14 may be expected to be arise from strain formed by stress at crack tip and it may be understood that the electric circuit method of this paper is an effective means to evaluate SCC growing process.

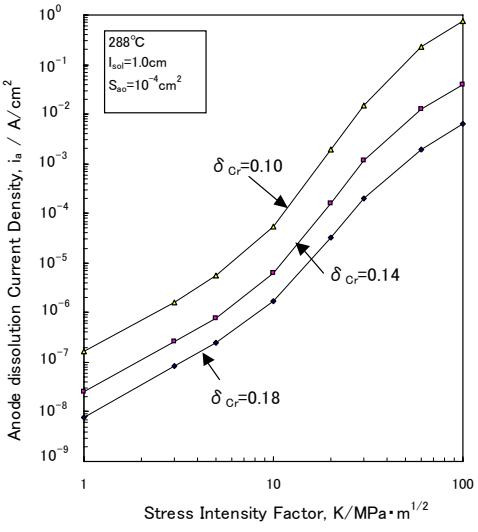

Fig. 14. K dependence of anode dissolution current density, i_a regarding δ_{Cr} of 0.18, 0.14 and 0.10 in 288℃high temperature water

4. Conclusions

The effects of stress factors on crack growth rate, da/dt of the sensitized 18-8 stainless steel in 288 ℃ high temperature water for SCC crack model of a bare surface at crack tip were quantitatively considered using 3 factors of ion flow passage area of solution (S_{sol}), dissolving cross section of metal (S_{met}) and total dissolving surface area of metal on the anode electrode (S_{dis}) and the following results were obtained.

(1) SCC crack growth rate may depend on both stress intensity factor, K and crack depth when S_{met} is equal to S_{sol}, and it may depend on both stress intensity factor, K and applied stress when S_{met} is constant.

(2) The calculated relation between da/dt and K was successfully identical with guideline curves in the literatures.

(3) The calculated curves regarding da/dt vs. K had lower limit and upper limit of da/dt. The upper limit may depend on degree of sensitization, equilibrium constant of hydrolysis reaction due to Cr^{3+} ions and standard electrode potential.

(4) The values of da/dt may fluctuate over 1 order to the same K value.

(5) In case CT specimen is used to measurement of SCC crack growth rate, the difference of distance between a point of application of force and the end of starter notch (starting point of fatigue crack) may influence SCC crack growth rate.

(6) The calculated anode dissolution current density at crack tip attains to the high levels of 10^{-2} to 1 A/cm^2 at larger K value such as 100 MPa · m$^{1/2}$. This calculated

current density is near those proposed by T.P. Hoar.

References

1. Y. Tsukaue, Proc. of the 53rd Japan conference on materials and environments (Akita), p.461 (2006).
2. Y. Tsukaue, The 14th Asian-Pacific Corrosion Control Conference (Shanghai), Paper No.06-08 (2006).
3. Roger W. Staehle, Proc. of the second international conference on ESCCD 2001(Hiroshima), p.8 (2001).
4. A. Turnbull, *Corrosion*, **57**, 175 (2001).
5. Y. Tsukaue, Proc. of the second international conference on ESCCD 2001(Hiroshima), p.366 (2001).
6. Y. Tsukaue, Proc. of JSCE materials and environments 2007(Tokyo), 2007(to be published).
7. H. Hirano, etc., Boshoku-Gijutsu, **31**, 517 (1982).
8. Thermal and Nuclear Power Engineering Society, JBWR-VIP-04 (2001).
9. W. S. Hazelton, W.H. Koo., NRC NUREG-0313 Rev.2 (1988).
10. EPRI, NP-4947-SR (1987)
11. S. Suzuki, etc., Proc. of JSCE Materials and Environments 2000(Yokohama), p.35 (2000).
12. F. P. Ford and M.J.Povich, *Corrosion*, **35**, 569 (1979).
13. T. Masuoka, etc., Proc. of JSCE Materials and Environments 2006(Tsukuba), p.67 (2006).
14. N. Otani, "Kinzoku-no-Sosei-to-Fushokuhanno", Sangyotosho, p.92 (1974).
15. T. P. Hoar and J.M. West, Nature, **181**, 835 (1958).
16. T. P. Hoar, Corrosion, **19**, 331t (1963).
17. K. Sugimoto and S. Soma, Boshoku Gijutsu, **31**, 574 (1982).
18. K. Fujiwara, etc., Boshoku Gijutsu, **30**, 270 (1981).